Desalination and Water Treatment
www.deswater.com
doi: 10.5004/dwt.2023.29947

312 (2023) 39–49
November

Effect of the SBA-15 N-functionalization on the adsorption of organic contaminants

A. Derylo-Marczewska[a,*], M. Zienkiewicz-Strzalka[a], K. Kusmierek[b], K. Skrzypczynska[b], A. Swiatkowski[b]

[a]*Department of Physical Chemistry, Institute of Chemical Sciences, Faculty of Chemistry, Maria Curie-Sklodowska University, Maria Curie-Sklodowska Sq. 3, 20-031 Lublin, Poland, email: anna.derylo-marczewska@mail.umcs.pl (A. Derylo-Marczewska)*
[b]*Institute of Chemistry, Military University of Technology, Kaliskiego 2, 00-908 Warsaw, Poland*

Received 9 June 2023; Accepted 31 August 2023

ABSTRACT

This work aimed to investigate the adsorption of selected organic molecules as models of water contaminants on unmodified and N-functionalized mesoporous silica adsorbents. In particular, ibuprofen and 4-chloro-2-methylphenoxyacetic acid (MCPA) were chosen as organic adsorbates. The surface of the mesoporous ordered silica phase containing free silanol groups was enriched with (3-aminopropyl)triethoxysilane by post-synthesis functionalization. The textural properties of synthesized silica phases were evaluated by low-temperature nitrogen adsorption–desorption isotherms, X-ray diffraction, scanning and transmission electron microscopy, infrared spectroscopy as well as thermal analysis. The SBA-15 type ordered mesoporous silica functionalized with amino groups (SBA-15_NH_2) was used as the highly porous adsorbent for analyzing the carrier-drug interactions and mutual affinity. The adsorption experimental data were analyzed and well-fitted using the Freundlich, Langmuir, and Temkin isotherms. Ibuprofen was better adsorbed on SBA-15 while MCPA showed greater adsorption affinity for SBA-15_NH_2. The better adsorption of MCPA on the N-functionalized silica was the result of interactions (hydrogen bond formation) between SBA-15_NH_2 and the adsorbate molecule. The mesoporous silica phases were also tested as carbon paste electrode (CPE) modifiers. Electrochemical measurements were conducted using cyclic voltammetry and differential pulse voltammetry. The mechanism of the electrooxidation process was controlled by diffusion. Compared with the bare (graphite) electrode, the silica-modified electrodes greatly increased the oxidation peak current of MCPA and ibuprofen. The peak current was strongly correlated with the adsorptive properties of the silica modifiers. The CPE modified by amino-functionalized SBA-15 type mesoporous silica (SBA-15_NH_2) showed a larger peak current and higher sensitivity for MCPA, while the CPE modified by pure silica phase electrode was much more appropriate for the detection of ibuprofen.

Keywords: SBA-15; (3-Aminopropyl)triethoxysilane (APTES); Adsorption; 4-Chloro-2-methylphenoxyacetic acid (MCPA); Ibuprofen

1. Introduction

The development of civilization determines the technological progress where new types of materials, as well as the improvement of known and applied solutions, are on the agenda. Continuous growth and economic success are associated with an increase in new threats, also on an environmental level. Sometimes there are risky situations where improving our well-being comes at the expense of the ecosystem and has negative effects on the natural biosphere. A fair and responsible approach to this issue should be a simultaneous search for solutions limiting the bioavailability of

* Corresponding author.

hazardous residues in nature. The organic substances and drug and pharmaceutical residues [1–3] next to nano-based technology waste [4–6], pesticides [7,8] surfactants [9], petroleum hydrocarbons [10], phenols [11], chlorinated biphenyls [12], and heavy metals pose a major ecological problem and require immediate attention. Recently, the production of adsorption systems has become a key idea with the hope that in specific applications they can replace traditional materials increasing the selectivity and efficiency of the technological processes. In this regard, silica materials based on mesoporous ordered phases (SBA-15) are being considered. To this day, this material is one of the most popular mesoporous silica. It belongs to amorphous silica containing cylindrical hexagonal pores and micropores in the silica walls. SBA-15 mesoporous silica phase has been investigated as a functional drug carrier system due to its predictable and repeatable properties [13,14]. In this case, the drug release control requirements were achieved and confirmed. Unwavering interest is the result of exceptional construction and neutrality towards living organisms. Additionally, this material does not show toxic and irritating effects and thus it is safe for human health. Limited surface chemistry is not an obstacle due to the existing possibilities of its modification and expansion of the surface layer with the desired functionality [15]. The functionalization of the surface makes the material suitably adapted to the specific application procedure by adjusting its physicochemical properties. The unmodified silica surface is mainly covered with silanol groups (–Si–OH), which makes it negatively charged. Therefore, joining the negatively charged molecules, biomolecules or modifiers is limited. To solve this problem and increase its bioavailability the modification of the surface by changing the surface charge should be performed. For modification, various types of trialkoxyorganosilanes functionalized with functional groups such as an amine (–NH_2 groups from 3-aminopropyltriethoxysilane) [16,17], mercapto (–SH groups from 3-mercaptopropyltrimethoxysilane) [18], ethenyl (–CH=CH_2 groups from vinyltrimethoxysilane) [19], diphenylphosphino (–PPh_2 from 4-(diphenylphosphine)phenyl triethoxysilane) [20] and many others may be applied. Among the possible methodology, the incorporation of amino groups seems to be the most reasonable solution with the greatest application possibilities. Advantages of surface functionalization include an increase of the adsorption capacity to the adsorbed substances, stabilization of the desorption process, the possibility of the controlled location of adsorbed substance, the concentration of desired components (for example during SPE procedure), and selective binding of adsorbates with the solid surface. Moreover, the surface modification by amine groups generates a terminal functional group with alkaline adsorption centers, desired during the adsorption of the substance with acidic properties. Such modification seems to be advisable in the case of adsorption of biologically active compounds from the group of propionic acid derivatives with anti-inflammatory, analgesic, and antipyretic properties (ibuprofen) or chemicals such as phenoxy herbicide compounds (MCPA, 4-chloro-2-methylphenoxyacetic acid). As an example of chemicals with acidic properties, an affinity for groups with basic properties should be expected (pK_a for ibuprofen equals to 5.2 and MCPA ~ 3.31). The topic of selected organic compounds' adsorption on silica material is significant and carries high application potential. Until now, the SBA-15-ibuprofen systems were tested as drug delivery practices. Here both, methods for incorporation of ibuprofen into the mesoporous silica phase and their release from the surface were investigated [21–24]. In the case of MCPA molecule, the SBA-15 carrier was tested as the support of a functional catalyst during the hydrochlorination of MCPA herbicide [25] and also as a selective adsorbent of this chlorinated aromatic compound [26]. In similar research, the achievements in the methods of quantification of this substance in the analysis of adsorption systems should be emphasized [27]. In this work, the surface modification of ordered mesoporous silica with the use of appropriate trialkoxysilanes was performed to generate efficient adsorption centers adopted to binding organic substances of global ecological importance. A critical approach to the obtained data made it possible to assess the affinity of selected organic systems to the primary and functionalized silica surface.

2. Experimental set-up

2.1. Reagents and materials

Self-assembly matrix agent Pluronic P123 (poly(ethylene oxide)-poly(propylene oxide)-poly(ethylene oxide)) ($EO_{20}PO_{70}EO_{20}$, M_w = 5,800) triblock copolymer), tetraethyl orthosilicate (TEOS, 98%) and (3-aminopropyl)triethoxysilane (APTES) were purchased from Sigma-Aldrich (St. Louis, MO, USA). Toluene (min. 99.5%) and hydrochloric acid (min. 35%–38%) as well as Na_2SO_4 were obtained from Avantor Performance Materials (Gliwice, Poland). The analytical grade ibuprofen (99%) and 2-methyl-4-chlorophenoxyacetic acid (98%), as well as graphite powder (diameter < 45 μm), were received from Sigma-Aldrich (St. Louis, MO, USA). The high-purity mineral oil (Nujol) used in the preparation of the carbon paste electrodes was obtained from Fluka (Buchs, Switzerland).

2.2. Synthesis of materials

The SBA-15 silica was synthesized according to the general procedure following the literature guidelines without unnecessary modifications [28]. In a typical synthesis, 4.0 g of P123 was dispersed in 120 mL of water and 9.12 g of 2 M HCl solution at 35°C while stirring. After 3 h, 8.54 g of TEOS was added to the mixture with continuous stirring at 35°C for 24 h. For stabilization, the solution was transferred to a Teflon inset equipped autoclave and maintained at 90°C for 48 h. After cooling, the solid product was filtered and calcined in air at 550°C for 5 h. The prepared SBA-15 product was functionalized by amine functional groups in a post-grafting process. For this 3.0 g of the dried SBA-15 powder was placed in a round-bottom flask with 50 mL of toluene and an appropriate amount of (3-aminopropyl) triethoxysilane. The amount of silane coupling agent was estimated at close to full monolayer covering by amine functional groups (0.6 mmol/g). The resultant mixtures were stirred and refluxed at 110°C for 3 h. Finally, the materials were washed with ethanol and vacuum dried at 100°C for 12 h to obtain functionalized mesoporous silica marked as SBA-15_NH_2.

2.3. Measurements and calculations

The textural properties of the initial and functionalized mesoporous silica materials were analyzed by measuring N_2 adsorption/desorption isotherms at 77 K over the full range of relative pressures by the automatic Micromeritics ASAP 2020 device. Specific surface areas (S_{BET}) were computed from experimental isotherms by applying the BET theory (Brunauer–Emmett–Teller) and linear range of experimental adsorption data at relative pressures of (P/P_0) 0.035–0.31, where P and P_0 denote the equilibrium and saturation pressures of nitrogen, respectively. The total pore volumes (V_{total}) were obtained from the adsorption value at the relative pressure P/P_0 ~ 0.99. The micropores' characteristics (surface area of micropores ($S_{BET\ MIC}$), micropores volume (V_{mic})) were obtained from the *t*-plot theory [29]. Pore-size distribution functions (PSD) of silica samples were calculated using Horvath–Kawazoe (HK) method (cylinder pore geometry by Saito–Foley) and non-local density functional theory (NLDFT) method using the theoretical model: Model: N_2@77K, for cylindrical pores in an oxide surface. The method is based on non-negative regularization: 0.00010 and standard deviation of fit: 2.95 cm^3/g of STP. Moreover, the calculations of pore size distributions followed the Barrett–Joyner–Halenda (BJH) procedure were applied. All samples were outgassed before analysis at 100°C for 24 h in the degas port of the analyzer. The dead space volume was measured for calibration on experimental measurement using helium as an adsorbate.

For the identification of the functional groups on the silica surface, photoacoustic spectroscopy analysis/Fourier-transform infrared spectroscopy (PAS/FTIR) was performed. Photoacoustic measurements as Fourier-transform infrared photoacoustic spectroscopy were performed using the Bio-Rad Excalibur 3000MX spectrometer equipped with the photoacoustic detector MTEC 300 in the range of 400–4,000 cm^{-1}.

X-ray photoelectron spectroscopy (XPS) data were collected on Multi-Chamber UHV System, Prevac (2009) using the hemispherical analyzer Scienta R4000 by monochromatic Al Kα radiation from high-intensity source MX-650, Scienta. All of the binding energies were calibrated by the C1s peak.

Thermal analysis of investigated materials was investigated using an STA 449 Jupiter F1 instrument (Netzsch, Germany). The measurements in the synthetic air atmosphere (50 cm^3/min) at a temperature range of 30°C–800°C were carried out with a heating rate of 10°C/min. The standard Al_2O_3 crucible and thermocouple of type S as a TG-DSC sensor were applied. The gaseous products released during thermal decomposition were analyzed by correlated FTIR spectrometer (Bruker, Germany).

The Small-Angle X-ray Scattering (SAXS) analysis was realized by an Empyrean diffractometer (PANalytical) with CuKα radiation using the SAXS/WAXS stage and capillary sample mode. The SAXS configuration includes a 2θ range of 0.13–4 degrees of 2θ, generator settings of 40 kV and 40 mA, and reflection geometry. The measurement was conducted in a single scan mode. The incident beam path consisted of a line focus type, W/Si, graded X-ray mirror with an elliptic shape. The diffracted beam path includes beam attenuator Cu 0.2 mm, PIXcel1D detector, and receiving slit with 0.05 mm active length. The length of the scattering vector (or scattering vector) θ is defined as $q = 4\pi\sin\theta/\lambda$, where 2θ the scattering angle, λ is the X-ray wavelength (1.5418 Å).

Transmission electron microscopy (Tecnai G2 T20 X-TWIN) was used to record the ordered morphology and the mesoporosity of silica. For this study, the samples were prepared by placing a drop of ethanol suspension of SBA-15 onto a carbon-coated copper grid, drying it in the air, and then transferring the grid to the microscope operated at an accelerated voltage of 200 kV.

2.4. Adsorption experiments

For the adsorption test, a certain amount of adsorbent (SBA-15 or SBA-15_NH_2) was added to Erlenmeyer flasks with different concentrations of ibuprofen or MCPA solution (10–100 μmol/L), and the flasks were shaken for 24 h at 150 rpm. The natural (original) pH of the adsorbate solutions (~4.5 for ibuprofen and ~4.1 for MCPA) was selected for the adsorption studies. After adsorption, the mixtures were filtered through filter paper, and the supernatant was measured by high-performance liquid chromatography with UV detection (Shimadzu LC-20, Kyoto, Japan). The measurements were conducted under isocratic conditions on a Luna C18 (4.6 × 150 mm, 3 μm) column (Phenomenex, Torrance, CA, USA) operated at 30°C. The mobile phase was a 50/50 (v/v) mixture of acetonitrile and water adjusted to pH 3.0 with acetic acid, the flow rate was set at 0.25 mL/min and the peaks were monitored at λ = 222 nm (ibuprofen) and λ = 278 nm (MCPA), respectively. The concentration of ibuprofen and MCPA was determined using the standard calibration curve which was obtained by plotting the peak area against the analyte concentration. The obtained calibration curves were linear with high R^2 correlation coefficients (≥0.998) and the equations for the regression line were $y = 1.691x - 0.056$ for ibuprofen and $y = 0.226x + 0.023$ for MCPA (where y is the peak area and x is the concentration of the analyte).

The equilibrium adsorption q_e (μmol/g) was calculated by Eq. (1):

$$q_e = \frac{(C_0 - C_e)V}{m} \tag{1}$$

where C_0 and C_e are the concentrations of ibuprofen or MCPA (μmol/L) before and after adsorption, respectively, V is the volume of the aqueous solution in the flask (L) and m denotes the mass of adsorbent (g).

2.5. Electrochemistry

The voltammetric measurements were carried out in a thermostated glass cell (0.04 L) at room temperature, in a three-electrode system. A carbon paste electrode was used as a working electrode. The reference electrode was a saturated calomel electrode and the counter electrode was a Pt wire. The differential pulse voltammetry (DPV) measurements were performed in an AutoLab potentiostat/galvanostat (model PGSTAT 20, Eco Chemie B.V., Utrecht,

The Netherlands) connected to a desktop computer and controlled by GPES 4.9 software. All the voltammograms were registered from 0 to +1.0 V at a sweep rate of 50 mV/s; the pulse height and width were set as 50 mV and 50 ms, respectively. The sampling time was 50 ms. The peak height was evaluated by the GPES software. The fabrication of the carbon paste electrode and the modified carbon paste electrodes: the carbon paste electrode was prepared by thoroughly mixing graphite powder and paraffin oil in a mortar with a pestle; the modified carbon paste electrodes were prepared in the same manner by precisely mixing weighed amount (10% wt.) of the SBA-15 or SBA-15_NH_2 with graphite powder and paraffin oil. The mixture was kept at 25°C for 3 d in a desiccator. After that, the paste was packed into the electrode cavity (2 mm) with Ø 3 mm. Before each use, the electrode surface was smoothed with a piece of paper until a smooth surface was observed.

Before the DPV measurements, the influence of the accumulation time on the peak current was determined for ibuprofen and MCPA in 0.1 mol/L Na_2SO_4 solution. Accumulation time was varied from 1 to 8 min. The experiments were conducted at the carbon paste electrodes (CPEs) containing 10% of mesoporous materials.

3. Results and discussion

3.1. Characterization

The properties of the porous structure are significant if the materials are applied as specific adsorbents and materials customized to sorption applications. Thus, the nitrogen adsorption/desorption isotherms as a crucial step were analyzed for the initial and functionalized mesoporous silica samples and presented in Fig. 1A. The differences in the isotherms course and nitrogen uptake reflect an essential variation of porous structure parameters presented in Table 1. According to the IUPAC classification, the type IV of isotherms with a Hl hysteresis loop was marked for both silica and functionalized silica samples. The adsorption isotherms exhibit a steep increase of nitrogen uptake at low relative pressures corresponding to the micropores filling. Although the presence of micropores was confirmed for the material before and after functionalization, pores quantitative characteristics indicate a decrease of this type of porosity after the functionalization step, which is directly reflected in a smaller jump in the nitrogen adsorbed quantity in the initial range of the isotherm (Fig. 1A). A general reduction of the adsorbed content resulting in a lower course of the experimental isotherm for the functionalized sample means a reduction in the available specific surface area. As a result of functionalization, the specific surface area (S_{BET}) decreased by nearly 38% from 890 to 555 m^2/g. The particularly sensitive to functionalization were micropores, which surface area decreased by almost 68% from 390 to 125 m^2/g. Both the total pore volume and the micropore volume were reduced due to the introduction of amino groups on the silica surface. The restriction in the availability of pores is particularly evident in pore size distribution analysis. In the case of mesopores, a decrease in the intensity of the peaks of the pore size distribution function is observed. The decreasing number of micropores is significant and has a direct impact on the average dimension of available porosity. A detailed analysis of the change in the size and number of pores is presented in Fig. 1 by applying various methods of their description (BJH, HK, and NLDFT).

To determine the chemical functionality of the mesoporous silica surface, a discussion of the quality of surface functional groups should be performed. Moreover, the quality of functionalization by amino groups can be evaluated due to an unequivocal structural response. A Fourier transform infrared spectroscopy, and in particular, infrared spectroscopy with photoacoustic detection (Fourier-transform infrared/photoacoustic spectroscopy FTIR/PAS) seems to be very useful in this issue. Fig. 2A shows the experimental FTIR/PAS spectra of investigated materials. The spectra show the absorption bands assigned to the structure-sensitive vibrations between (SiO_4) tetrahedra at about 800 and 1,080 cm^{-1} signifying the typical symmetric and asymmetric stretching of Si–O–Si, respectively. The silanol groups are visible in the bending range of vibrations (~3,400 cm^{-1}). The involvement of silanol groups originally bound to the silica material was confirmed by changing their absorption properties. The surface properties were changed after functionalization. (Fig. 2B exhibits a narrow band at ~3,745 cm^{-1} for initial mesoporous ordered silica, which indicates the presence of isolated silanols. Next to this, extensively hydrogen-bonded silanols as broadband centered at 3,500 cm^{-1} are found. The absorption bands of amino groups in the IR spectra show a relatively low intensity, and additionally, they can be covered by stronger bands from other functional groups. On the IR spectra, primary amines with characteristic –NH_2 vibrations are visible in the 3,000–3,500 cm^{-1} range. The widening of a band should be assigned by the symmetric stretching vibration of N–H groups in the terminal amine groups cross-linked with the –SiOH groups. The vibrations for primary amines are observed in the range of 1,600–1,580 cm^{-1}. The direct evidence of the N–H bending vibration should be described by the peak at about 1,540 cm^{-1} as well as from a sharp leap at about 578 cm^{-1}. The bands at 1,646 and 970 cm^{-1} in the SBA-15 (very weak) and SBA-15_NH_2 samples illustrate the –OH deformation associated with the Si–OH groups. In both cases, these signals were significantly more intense for samples after functionalization.

Fig. 3 shows the XPS spectra of the silica and functionalized silica surfaces. The XPS data were also presented in Table 2. The survey scans were recorded in the region of binding energies of 0–1,200 eV (Fig. 3A). The high-resolution XPS analysis indicates the single O1s and Si2p core levels for both samples (Fig. 3B and C), as well as compound N1s signal for the SBA-15_NH_2 sample (Fig. 3D). O1s photopeak's reveal the negative shift of binding energy. The functionalization causes the incorporation of silanol chains around the silica particles and creates new chemical bonds between existing oxygen atoms and silicon from APTES. Here, the electronegativity of the doping element (Si from APTES) is lower than the base element, the electron density around oxygen atoms increases and the binding energy decreases, leading to a redshift in BE peak position. The shift of binding energy equals 0.7, (533.3 and 532.6 eV for SBA-15 and SBA-15_NH_2 materials, respectively).

Si2p core levels remain without significant changes after modification. It is expected, that nitrogen atoms can

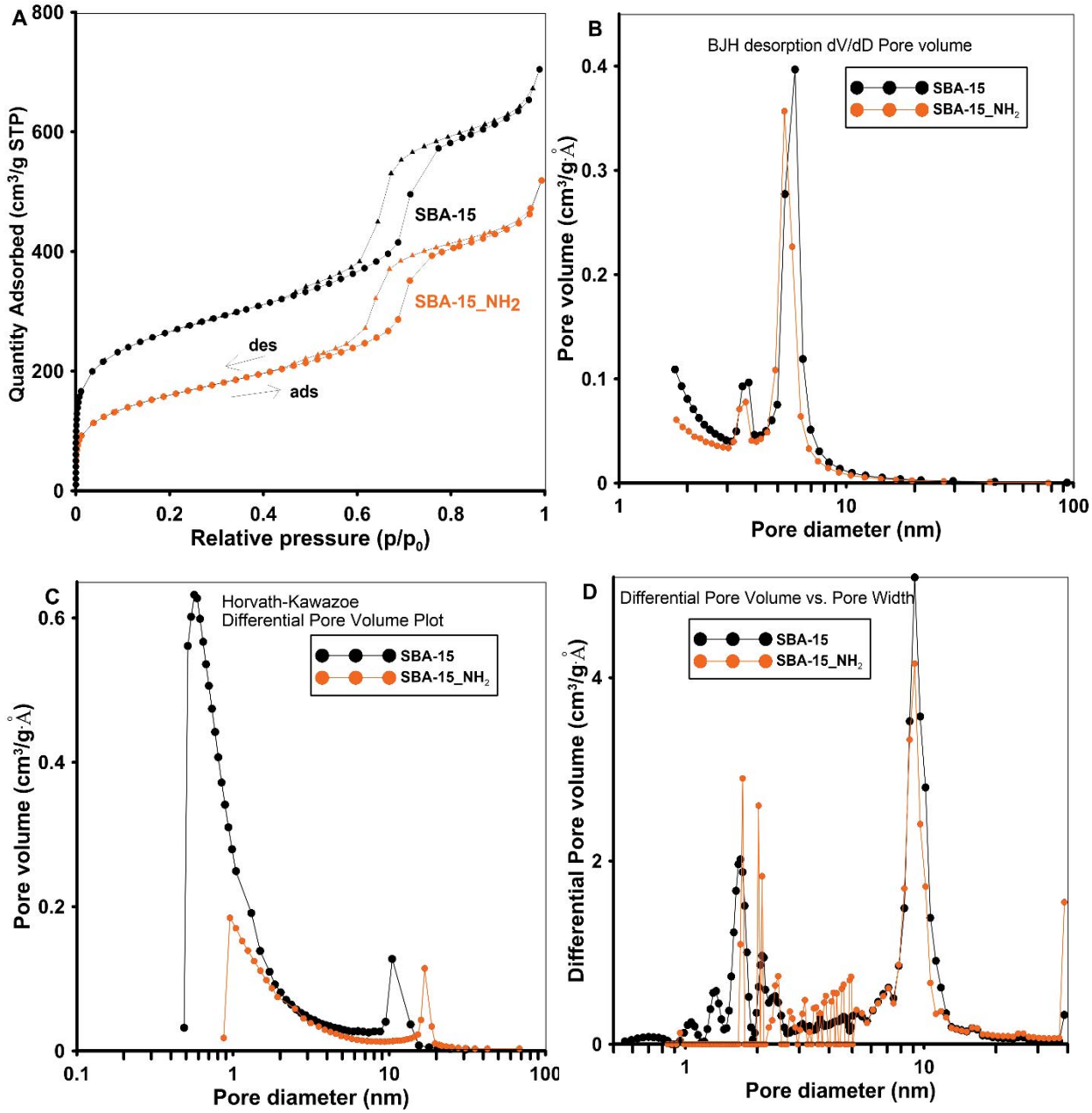

Fig. 1. (A) Nitrogen adsorption/desorption isotherms at 77 K for the initial (SBA-15) and functionalized mesoporous ordered silica (SBA-15_NH_2), (B) porosity distributions for both types by the Barrett–Joyner–Halenda with Halsey–Faas correction, (C) porosity distributions by the Horvath–Kawazoe calculations and (D) porosity distribution by density functional theory with model: N_2@77K, cylindrical pores in an oxide surface.

Table 1
Values of parameters characterizing the porous structure of adsorbents

Sample	Surface area (S_{BET}) (m^2/g)		Pore volume (cm^3/g)		Pore-size distribution (nm)		
	$S_{BET\ Total}$	$S_{BET\ MIC}$	V_{total}	V_{mic}	BJH[a]	HK[b]	NLDFT[c]
SBA-15	890	390	1.089	0.187	5.88	3.82	1.7, 10
SBA-15_NH_2	555	125	0.802	0.060	5.66	6.74	1.9, 10

[a]Barrett–Joyner–Halenda desorption average pore diameter (4V/A); [b]Horvath–Kawazoe median pore width; [c]Non-local density functional theory maximum mean peaks.

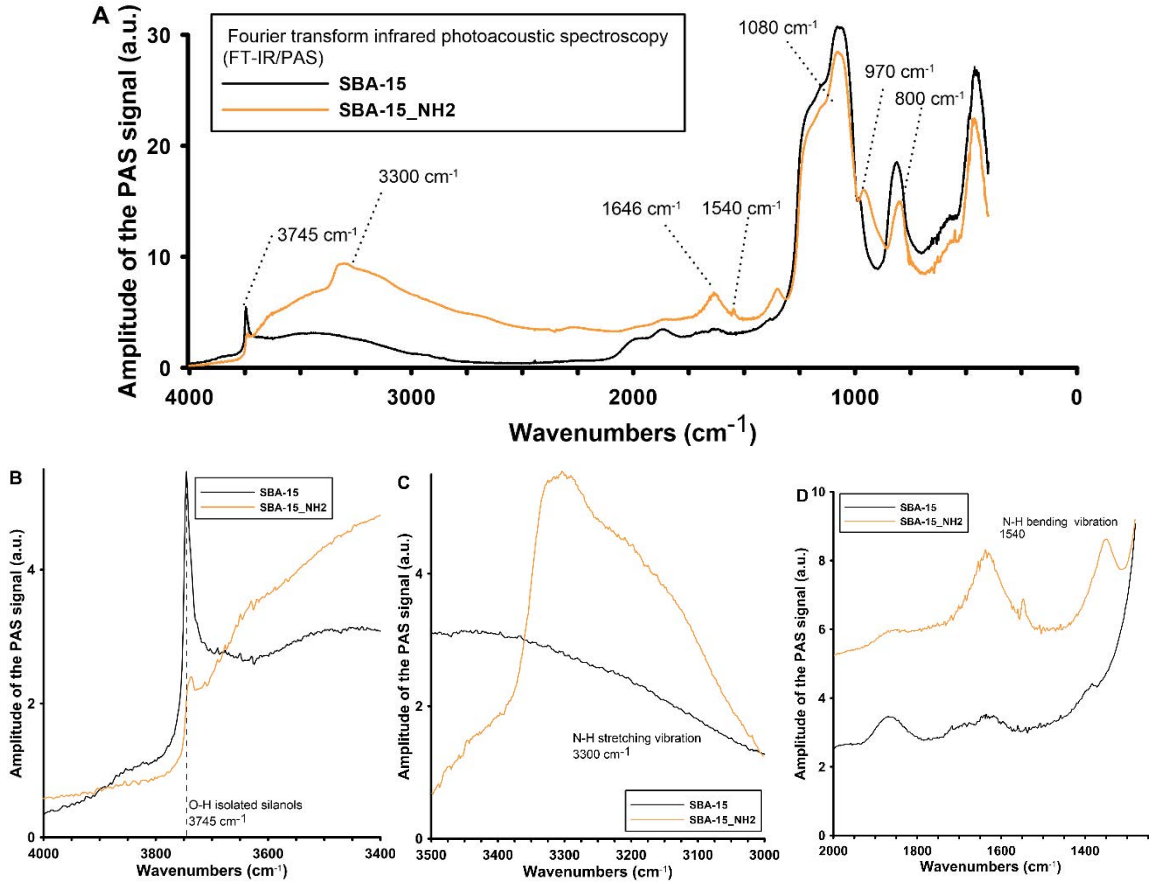

Fig. 2. (A) FTIR/PAS spectra of initial mesoporous silica (SBA-15) compared with functionalized mesoporous silica (SBA-15_NH_2) and (B–D) magnification of the selected areas of FTIR/PAS spectra.

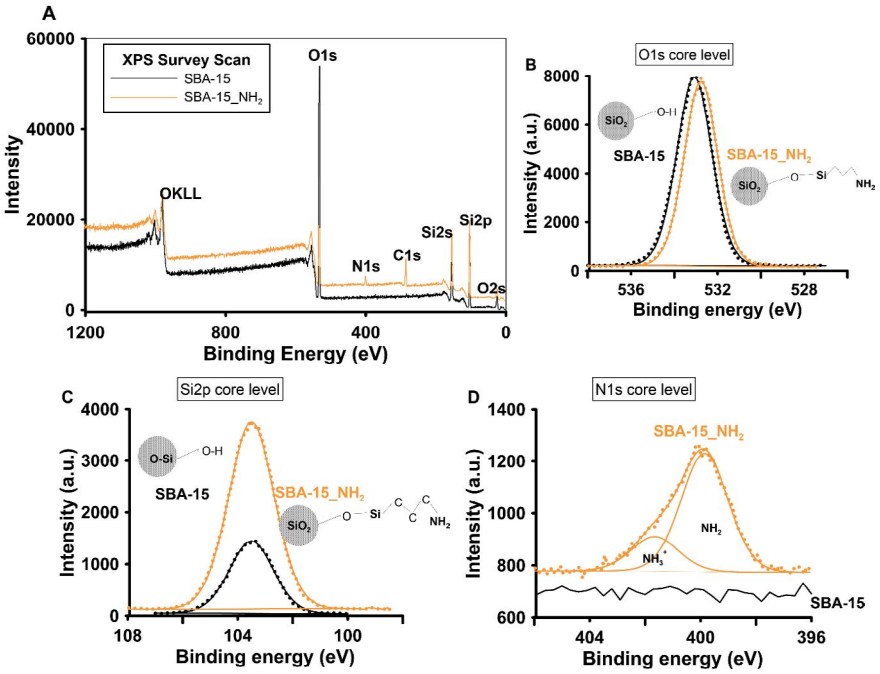

Fig. 3. X-ray photoelectron spectra of initial and amine-functionalized mesoporous silica materials: (A) survey scan and high-resolution X-ray photoelectron spectra of (B) O1s, (C) Si2p, and (D) N1s core levels.

Table 2
X-ray photoelectron spectroscopy data of mesoporous ordered silica

	Region	Position (eV)	FWHM	% At Conc.	% Mass Conc.	% St. Dev.
SBA-15	C1s	284.1	0.46	0.48	0.28	0.1
	O1s	533.3	2.35	59.33	45.55	0.2
	Si2p	103.4	2.43	40.19	54.17	0.2
SBA-15_NH_2	C1s	285.5	3.03	12.5	7.6	0.2
	O1s	532.6	2.43	48.6	39.2	0.2
	Si2p	103.5	2.52	36.3	51.4	0.2
	N1s[a]	401	3.32	2.6	1.9	0.1

[a]N1s high-resolution X-ray photoelectron spectroscopy scans of the SBA-15_NH_2 revealed two signals of N1sA and N1sB of two different chemical states of N1s (400 and 401.8 eV for NH_2 and NH_3^+ states, respectively).

exist in different oxidation states as –NH_2 and protonated –HN_3^+ species which influence the adsorption behavior relative to investigated adsorbates. NH_2 bonds are attributed to the binding energy at 400 eV, while positively charged –NH_3^+ groups are identified at higher binding energies (401.8 eV) [30].

The SAXS curves of SBA-15 and SBA-15_NH_2 samples confirm well-ordered mesoporous systems arranged as two-dimensional, hexagonal symmetry (*p6mm*) (Fig. 4A). Hexagonal symmetry and ordered structure of the pores are confirmed by three well-resolved peaks at small diffraction angles specified as (100) = 0.062 Å^{-1}, (110) = 0.110 Å^{-1} and (200) = 0.128 Å^{-1} for SBA-15 and (100) = 0.064 Å^{-1}, (110) = 0.114 Å^{-1} and (200) = 0.129 Å^{-1} for SBA-15_NH_2 sample, respectively. The unit cell parameters (a) were determined from these data as an average of unit-cell parameters defined for (100), (110), and (200) Bragg's peaks according to equations: $a_{100} = (2d_{100})/\sqrt{3}$, $a_{110} = 2d_{110}$, $a_{200} = (4d_{200})/\sqrt{3}$ and equals 114.8 Å for SBA-15 and 111.9 Å for SBA-15_NH_2.

The results of SAXS analysis are in line with the pore size diameter (the distance between two pores) from transmission electron microscopy images where the observed size equals ~60 Å as well as low-temperature N_2 sorption isotherms. After surface functionalization with amine groups, a reduction in the availability of the light of the carrier pores was observed by reducing their size.

The available porosity should be taken into account during analyzing the adsorption process of organic compounds with specific molecular sizes. The behavior of the active substance inside the formed mesopores should be also regarded and may also depend on the diameter and length of the inorganic channels. In this work, the relatively small molecular sizes of ibuprofen (Fig. 5A) and MCPA (Fig. 5B) make it possible for good penetration into even micropores of the support (depending on their availability).

3.2. Adsorption isotherms

The adsorption isotherms for ibuprofen and MCPA on SBA-15 and SBA-15_NH_2 are presented in Fig. 6.

The data were analyzed using Freundlich [Eq. (2)], Langmuir [Eq. (3)], and Temkin [Eq. (4)] isotherms [31]. The linear forms of the isotherms are given by Eqs. (2)–(4):

$$\ln q_e = \ln K_F + \frac{1}{n}\ln C_e \tag{2}$$

$$\frac{C_e}{q_e} = \frac{1}{q_m}C_e + \frac{1}{q_m K_L} \tag{3}$$

$$q_e = \frac{RT}{b_T}\ln A_T + \frac{RT}{b_T}\ln C_e \tag{4}$$

where K_F ((μmol/g)(L/μmol)$^{1/n}$) and n are the Freundlich adsorption constants, q_m (μmol/g) and K_L (L/μmol) are the Langmuir isotherm parameters, b_T (J/mol) is the Temkin constant related to the heat of adsorption, A_T (L/g) is the equilibrium binding constant corresponding to the maximum binding energy, T is the temperature (K) and R is the gas constant (8.314 J/mol·K).

The Freundlich, Langmuir, and Temkin isotherm parameters were calculated from the slope and intercept of the linear plots of lnq_e vs. lnC_e, C_e/q_e vs. C_e, and q_e vs. lnC_e, respectively, and are listed in Table 3.

As depicted in Table 3, all used adsorption isotherms, Freundlich, Langmuir, and Temkin, describe well the experimental systems (high correlation coefficients $R^2 \geq 0.913$–0.997). It is partly a result of a relatively narrow range of equilibrium adsorbate concentrations, in which various theoretical equations may be fitted well. Taking into account the uniform porous structure of synthesized materials one can expect that the studied adsorption systems may be regarded as homogeneous to a large extent. However, one should take into account that the created surface active centers can interact with adsorbate molecules in different ways.

Adsorption is a complex process that depends on the individual properties of the adsorbate and adsorbent. Both the textural properties of the adsorbent (its specific surface area, pore size distribution) and the chemical properties of the surface (the presence of surface functional groups) have a critical influence. Therefore, it can be expected that the modification of silica by APTES will change its adsorption capacity because it has caused changes in its surface chemistry and porous structure. As can be seen in Fig. 6 and Table 3, ibuprofen was adsorbed better on SBA-15 while MCPA showed greater adsorption affinity for SBA-15_NH_2. The better adsorption of MCPA on the N-functionalized silica was the result of interactions (hydrogen bond formation) between amino groups of SBA-15_NH_2 and the carboxyl group of herbicide molecule. Similar interactions

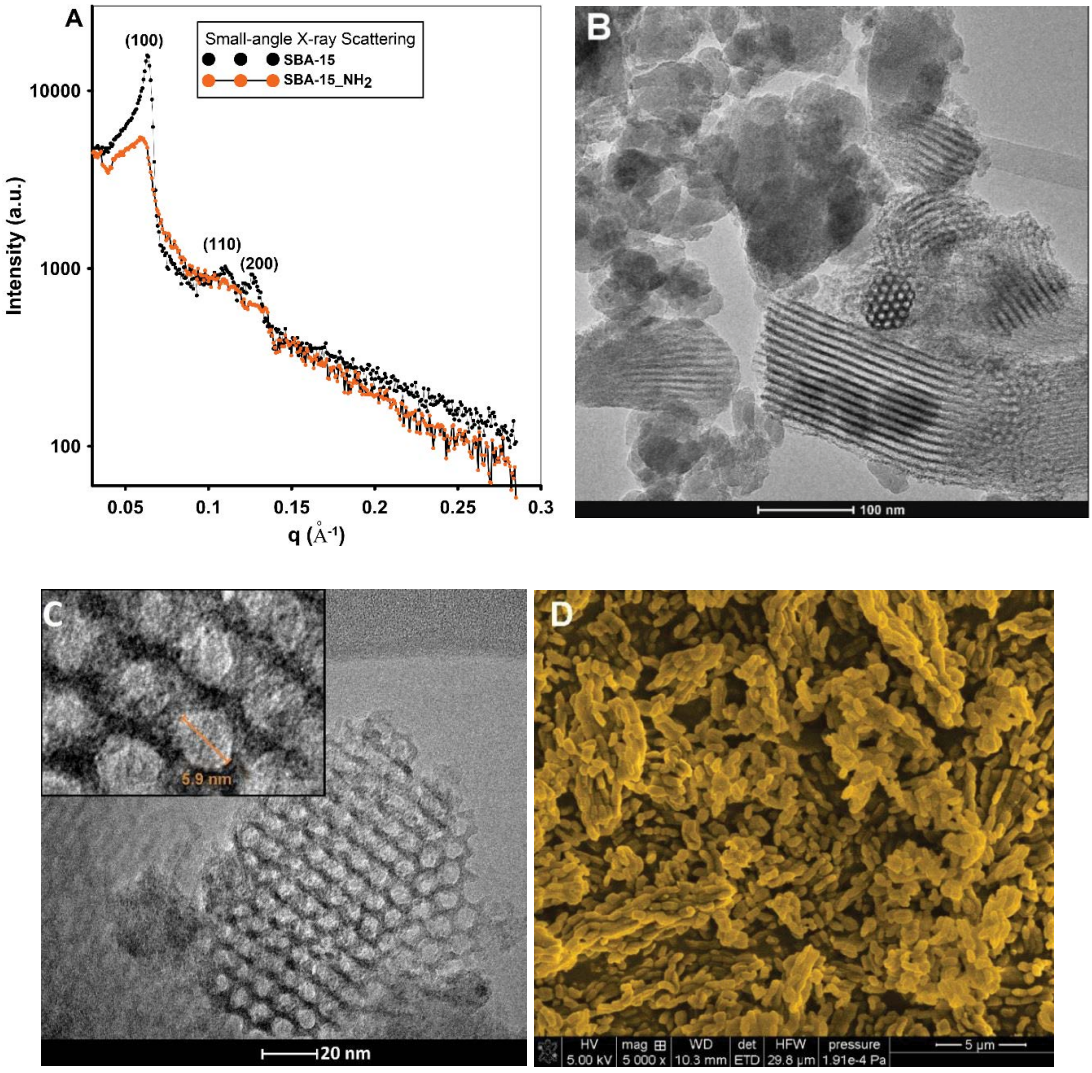

Fig. 4. Structure and morphology of initial and amine-functionalized mesoporous silica (A) experimental SAXS profiles of investigated samples, (B,C) transmission electron microscopy images of SBA-15 at various magnifications with the sizing of mesopores in the inset of Fig. 4C, and (D) scanning electron microscopy image of SBA-15_NH_2.

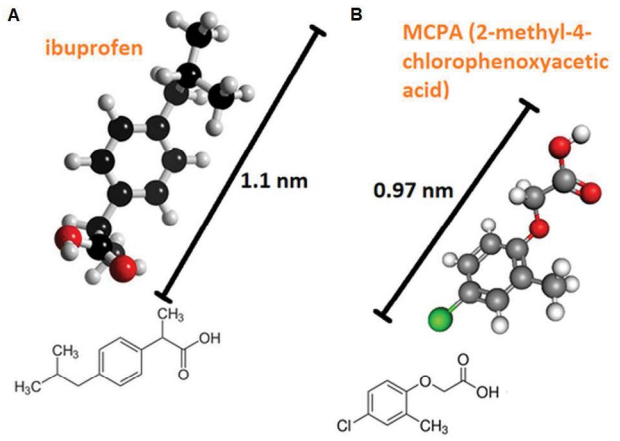

Fig. 5. Structure and molecular dimensions of two selected types of organic adsorbates: ibuprofen and MCPA.

were reported for the adsorption of 2,4-dichlorophenoxyacetic acid (2,4-D) on APTES-modified SBA-15 [26], mesocellular siliceous foam (MCF) [26], MCM-41 [32], hexagonal mesoporous silica [33], grafted mesoporous carbons [34] or carbon black [35]. The higher adsorption capacity of unmodified SBA-15 for ibuprofen was probably due to its higher specific surface area in comparison to the functionalized silica (890 vs. 555 m^2/g). The ibuprofen molecule also contains a carboxyl group, so hydrogen bonding interactions between the amino groups of SBA-15_NH_2 and the carboxyl groups of ibuprofen are possible [36,37] which, at least in theory, should significantly increase adsorption efficiency. However, in this work, the opposite results were observed – better adsorption of ibuprofen on unmodified silica. Szegedi et al. [38] studied the adsorption of ibuprofen on amino-modified MCM-41 and SBA-15 silica materials. They found that in contrast to MCM-41, the APTES-modified SBA-15 adsorbed a lower amount of

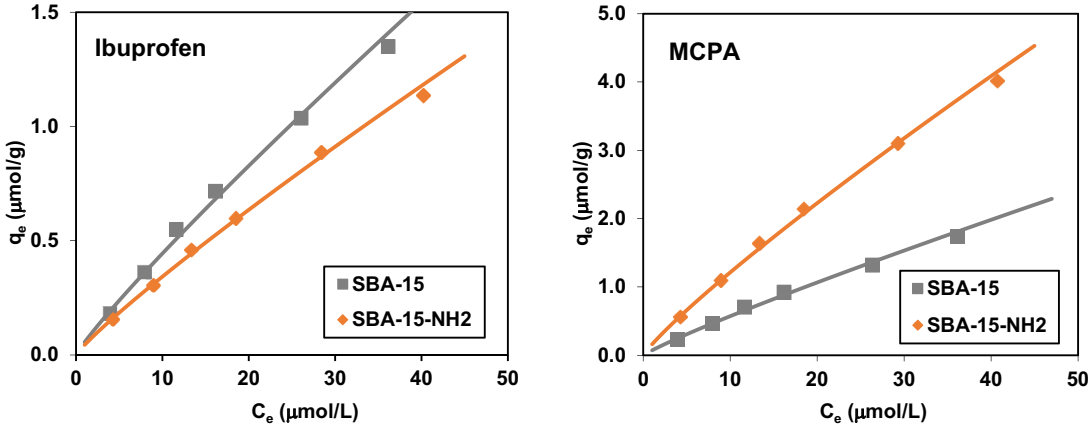

Fig. 6. Adsorption isotherms of ibuprofen and MCPA on the mesoporous silica (line: fitting of Freundlich isotherm).

Table 3
Freundlich, Langmuir and Temkin isotherm constants for adsorption of ibuprofen and MCPA on the mesoporous ordered silica materials

Adsorption isotherm	adsorbent/adsorbate			
	SBA-15		SBA-15_NH$_2$	
	IBU	MCPA	IBU	MCPA
Freundlich isotherm				
K_F (µmol/g)(L/µmol)$^{1/n}$	0.056	0.073	0.044	0.162
$1/n$	0.899	0.895	0.891	0.875
R^2	0.995	0.995	0.998	0.997
Langmuir isotherm				
q_m (µmol/g)	5.551	6.891	4.660	14.49
b (L/µmol)	0.014	0.013	0.024	0.016
R^2	0.921	0.913	0.968	0.954
Temkin isotherm				
b_T (J/mol)	4.745	3.709	5.680	1.630
A_T (L/g)	0.288	0.883	0.261	0.265
R^2	0.947	0.939	0.935	0.945

ibuprofen. The authors observed that modification of SBA-15 by APTES caused a reduction in the BET surface area of the material due to the blocking of the micropores, where some of the silanol groups are located. Therefore, the amino groups in the micropores are inaccessible to larger molecules of ibuprofen, and, as a result, the adsorption capacity of modified SBA-15 decreases. Such a phenomenon, a different mechanism of adsorption of ibuprofen compared to MCPA, for example, *via* hydrophobic interaction between ibuprofen and SBA-15 surface and/or electron donor–acceptor interaction between oxygen on the siloxane surface of SBA-15 and π-system of ibuprofen [39] may be suggested.

3.3. Electrochemical studies

The mesoporous silica materials were also tested as carbon paste electrodes (CPE) modifiers. The effect of accumulation time on the peak current of ibuprofen compared to MCPA (50 µmol/L) is shown in Fig. 7.

The peak current increased with increasing accumulation time up to about 4 min and then became stable.

Electrochemical measurements were conducted using differential pulse voltammetry (DPV). Fig. 8 shows the DPV curves registered for 0.1 mmol/L ibuprofen and MCPA

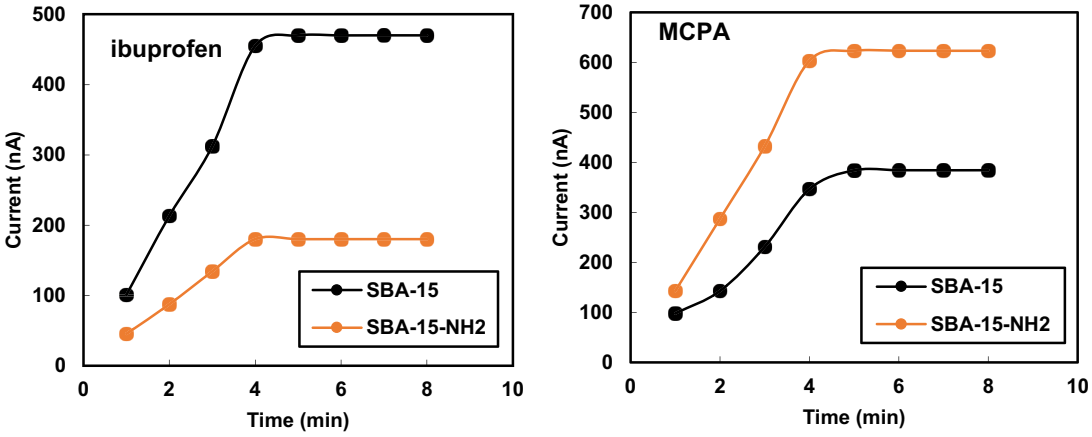

Fig. 7. Effect of accumulation time on the peak current of ibuprofen and MCPA in 0.1 mol/L Na_2SO_4 solution.

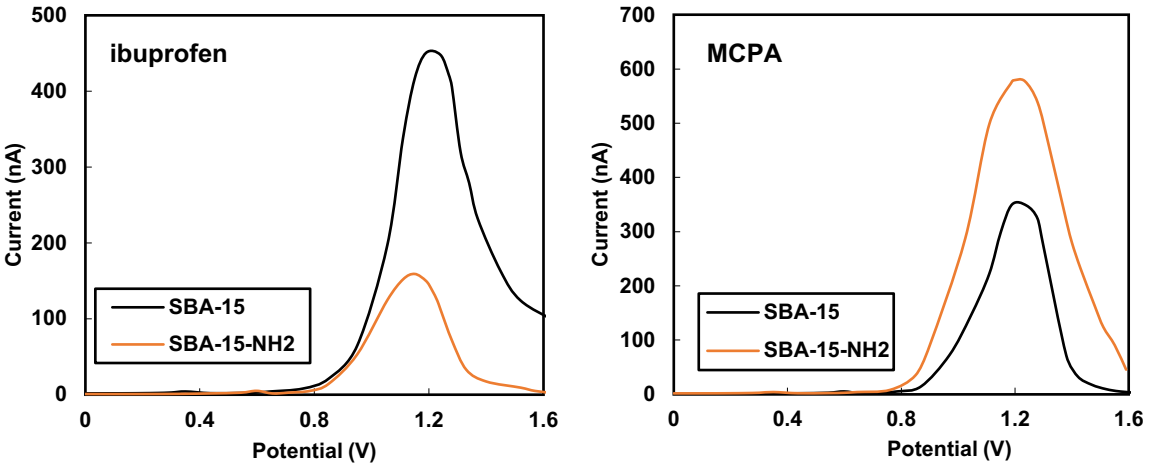

Fig. 8. Differential pulse voltammetry registered for 0.1 mmol/L ibuprofen and MCPA solutions using carbon paste electrodes containing 10% by mass of tested materials (SBA-15 and SBA-15_NH_2).

solutions using carbon paste electrodes containing 10% by mass of tested materials.

The mechanism of the electrooxidation process was controlled by diffusion. Compared with the bare (graphite) electrode, the silica-modified electrodes greatly increased the oxidation peak current of ibuprofen and MCPA, showing strong signal enhancement effects. The peak current was strongly correlated with the adsorptive properties of the silica materials used as modifiers. SBA-15_NH_2 modified CPE showed a larger peak current and higher sensitivity for MCPA (similarly as earlier was reported for 4-chlorophenol [40]), while the SBA-15 modified electrode was much more appropriate for the detection of ibuprofen.

4. Conclusions

In the paper, the adsorption of ibuprofen and 4-chloro-2-methylphenoxyacetic acid (MCPA) as model water contaminants on unmodified and N-functionalized mesoporous ordered silica SBA-15 was investigated. A mesoporous silica support with an ordered pore system and pronounced porosity was successfully modified with amino groups by the post-synthesis method improving the functionality of the surface. However, the modification deteriorated the textural properties of the material, including blocking access to the pore space and disturbing their structural order. As a result of the conducted adsorption studies, it was determined that in the case of MCPA, the adsorption was determined by the hydrogen bonding with electrostatic nature between the aminated surface of silica (–NH_3^+ groups at experimental pH (pH = 4.1) and below pH_{PZC} (pH_{PZC}~8.5 [41])) and dissociated carboxyl groups of MCPA ($^-$OOC-R groups above pKa (pKa~3.3) at experimental pH (pH = 4.1)). Unlike this system, the ibuprofen molecules with a slightly larger molecular size are screened from the system modified with amino groups, which limit the availability of pores and reduce the specific surface area. Both mesoporous silica were also tested as carbon paste electrodes (CPEs) modifiers in voltametric measurements. SBA-15_NH_2 modified CPE showed a larger peak current and higher sensitivity for MCPA while SBA-15 modified electrode was much more appropriate for the detection of ibuprofen. The peak current was strongly correlated with the adsorptive properties of the silica CPEs modifiers.

References

[1] S.R. Hughes, P. Kay, L.E. Brown, Global synthesis and critical evaluation of pharmaceutical data sets collected from river systems, Environ. Sci. Technol., 47 (2013) 661–677.
[2] T. Aus der Beek, F.-A. Weber, A. Bergmann, S. Hickmann, I. Ebert, A. Hein, A. Küster, Pharmaceuticals in the environment – global occurrences and perspectives, Environ. Toxicol. Chem., 35 (2016) 823–835.
[3] J.M. Brausch, K.A. Connors, B.W. Brooks, G.M. Rand, Human pharmaceuticals in the aquatic environment: a review of recent toxicological studies and considerations for toxicity testing, Rev. Environ. Contam. Toxicol., 218 (2012) 1–99.
[4] C. Bressot, N. Manier, C. Pagnoux, O. Aguerre-Chariol, M. Morgeneyer, Environmental release of engineered nanomaterials from commercial tiles under standardized abrasion conditions, J. Hazard. Mater., 322 (2017) 276–283.
[5] T.V. Duncan, K. Pillai, Release of engineered nanomaterials from polymer nanocomposites: diffusion, dissolution and desorption, ACS Appl. Mater. Interfaces, 7 (2015) 2–19.
[6] D.M. Mitrano, E. Rimmele, A. Wichser, R. Erni, M. Height, B. Nowack, Presence of nanoparticles in wash water from conventional silver and nano-silver textiles, ACS Nano, 8 (2014) 7208–7219.
[7] I. Mahmood, S.R. Imadi, K. Shazadi, A. Gul, K.R. Hakeem, Effects of Pesticides on Environment, K. Hakeem, M. Akhtar, S. Abdullah, Eds., Plant, Soil and Microbes, Springer, Cham, 2016, pp. 253–269.
[8] I.M. Meftaul, K. Venkateswarlu, R. Dharmarajan, P. Annamalai, M. Megharaj, Pesticides in the urban environment: a potential threat that knocks at the door, Sci. Total Environ., 711 (2020) 134612, doi: 10.1016/j.scitotenv.2019.134612.
[9] A.A. Siyal, M.R. Shamsuddin, A. Low, N.E. Rabat, A review on recent developments in the adsorption of surfactants from wastewater, J. Environ. Manage., 254 (2020) 109797, doi: 10.1016/j.jenvman.2019.109797.
[10] A. Truskewycz, T.D. Gundry, L.S. Khudur, A. Kolobaric, M. Taha, A. Aburto-Medina, A.S. Ball, E. Shahsavari, Petroleum hydrocarbon contamination in terrestrial ecosystems-fate and microbial responses, Molecules, 24 (2019) 3400, doi: 10.3390/molecules24183400.
[11] A. Kahru, A. Maloverjan, H. Sillak, The toxicity and fate of phenolic pollutants in the contaminated soils associated with the oil-shale industry, Environ. Sci. Pollut. Res., 9 (2002) 27–33.

[12] A. Beyer, M. Biziuk, Environmental fate and global distribution of polychlorinated biphenyls, Rev. Environ. Contam. Toxicol., 201 (2009) 137–158.
[13] J.S. Beck, J.C. Vartuli, J. Roth, M.E. Lenowicz, C.T. Kresge, K.D. Schmidt, C.T.W. Chu, D.H. Olson, E.W., S.B. Sheppard McCullen, J.B. Higgins, J.L. Schlenker, A new family of mesoporous molecular sieves prepared with liquid crystal templates, J. Am. Chem. Soc., 114 (1992) 10834–10843.
[14] D.Y. Zhao, J.L. Feng, Q.S. Huo, Triblock copolymer syntheses of mesoporous silica with periodic 50 to 300 angstrom pores, Science, 279 (1998) 548–552.
[15] J.D. Webb, T. Seki, J.F. Goldston, M. Pruski, C.M. Crudden, Selective functionalization of the mesopores of SBA-15, Microporous Mesoporous Mater., 203 (2015) 123–131.
[16] M.A.S. Chong, X.S. Zhao, Functionalization of SBA-15 with APTES and characterization of functionalized materials, J. Phys. Chem. B, 107 (2003) 12650–12657.
[17] L.M.O. Ribeiro, L.N.S.S. Falleiros, M.M. de Resende, Immobilization of the enzyme invertase in SBA-15 with surfaces functionalized by different organic compounds, J. Porous Mater., 26 (2019) 77–89.
[18] A.M. Liu, K. Hidajat, S. Kawi, D.Y. Zhao, A new class of hybrid mesoporous materials with functionalized organic monolayers for selective adsorption of heavy metal ions, Chem. Commun., 13 (2000) 1145–1146.
[19] Q. Wei, H.Q. Chen, Z.R. Nie, L.I. Hao, Y.L. Wang, Q. Li, J.X. Zou, Preparation and characterization of vinyl-functionalized mesoporous SBA-15 silica by a direct synthesis method, Mater. Lett., 61 (2007) 1469–1473.
[20] J. Huang, M. Wang, S. Zhang, B. Hu, H. Li, Influence of the Pd(II) coordination model on the catalytic performance of Pd–PPh_2–SBA-15 in C–C bond forming reactions, J. Phys. Chem., 115 (2011) 22514–22522.
[21] S.W. Song, K. Hidajat, S. Kawi, Functionalized SBA-15 materials as carriers for controlled drug delivery: influence of surface properties on matrix-drug interactions, Langmuir, 11 (2005) 9568–9575.
[22] I. Izquierdo-Barba, E. Sousa, J.C. Doadrio, A.L. Doadrio, J.P. Pariente, A. Martínez, M. Vallet-Regí, Influence of mesoporous structure type on the controlled delivery of drugs: release of ibuprofen from MCM-48, SBA-15 and functionalized SBA-15, J. Sol-Gel Sci. Technol., 50 (2009) 421–429.
[23] R. Mellaerts, J.A. Jammaer, M. Van Speybroeck, H. Chen, J.V. Humbeeck, P. Augustijns, J.A. Martens, Physical state of poorly water soluble therapeutic molecules loaded into SBA-15 ordered mesoporous silica carriers: a case study with itraconazole and ibuprofen, Langmuir, 24 (2008) 8651–8659.
[24] M. Ulfa, D. Prasetyoko, Drug loading-release behaviour of mesoporous materials SBA-15 and CMK-3 using ibuprofen molecule as drug model, J. Phys. Conf. Ser., 1153 (2019) 012065, doi: 10.1088/1742-6596/1153/1/012065.
[25] E. Diaz, A.F. Mohedano, J.A. Casas, C. Shalaby, S. Eser, J.J. Rodriguez, On the performance of Pd and Rh catalysts over different supports in the hydrodechlorination of the MCPA herbicide, Appl. Catal., B, 186 (2016) 151–156.
[26] M. Moritz, M. Geszke-Moritz, Application of nanoporous silica as adsorbents for chlorinated aromatic compounds. A comparative study, Mater. Sci. Eng. C, 41 (2014) 42–51.
[27] A. Białek, K. Skrzypczyńska, K. Kuśmierek, A. Świątkowski, Voltammetric determination of MCPA, 4-chloro-o-cresol and o-cresol in water using a modified carbon paste electrode, Int. J. Electrochem. Sci., 14 (2019) 228–237.
[28] D. Zhao, Q. Huo, J. Feng, B.F. Chmelka, G.D. Stucky, Nonionic triblock and star diblock copolymer and oligomeric surfactant syntheses of highly ordered, hydrothermally stable, mesoporous silica structures, J. Am. Chem. Soc., 120 (1998) 6024–6036.
[29] S.J. Gregg, K.S.W. Sing, Adsorption, Surface Area and Porosity, Academic Press, London, 1982.
[30] C.D. Wagner, A.V. Naumkin, A.K. Vass, J.W. Alisson, C.J. Powell, J.R.J. Rumble, NIST X-Ray Photoelectron Spectroscopy Database 20 Version 3.4, National Institute of Standards and Technology, Gaithersburg, MD, USA, 2003.
[31] M.A. Al-Ghouti, D.A. Da'ana, Guidelines for the use and interpretation of adsorption isotherm models: a review, J. Hazard. Mater., 393 (2020) 122383, doi: 10.1016/j.jhazmat.2020.122383.
[32] J. Ortiz Otalvaro, M. Avena, M. Brigante, Adsorption of organic pollutants by amine functionalized mesoporous silica in aqueous solution. Effects of pH, ionic strength and some consequences of APTES stability, J. Environ. Chem. Eng., 7 (2019) 103325, doi: 10.1016/j.jece.2019.103325.
[33] P. Patiparn, S. Takizawa, Effect of surface functional group on adsorption of organic pollutants on hexagonal mesoporous silicate, Water Sci. Technol. Water Supply, 6 (2006) 17–25.
[34] J. Goscianska, A. Olejnik, Removal of 2,4-D herbicide from aqueous solution by aminosilane-grafted mesoporous carbons, Adsorption, 25 (2019) 345–355.
[35] I. Legocka, K. Kuśmierek, A. Świątkowski, E. Wierzbicka, Adsorption of 2,4-D and MCPA herbicides on carbon black modified with hydrogen peroxide and aminopropyltriethoxysilane, Materials, 15 (2022) 8433, doi: 10.3390/ma15238433.
[36] E. Ahmadi, N. Dehghannejad, S. Hashemikia, M. Ghasemnejad, H. Tabebordbar, Synthesis and surface modification of mesoporous silica nanoparticles and its application as carriers for sustained drug delivery, Drug Delivery, 21 (2014) 164–172.
[37] N.H.N. Kamarudin, A.A. Jalil, S. Triwahyono, N.F.M. Salleh, A.H. Karim, R.R. Mukti, B.H. Hameed, A. Ahmad, Role of 3-aminopropyltriethoxysilane in the preparation of mesoporous silica nanoparticles for ibuprofen delivery: effect on physicochemical properties, Microporous Mesoporous Mater., 180 (2013) 235–241.
[38] A. Szegedi, M. Popova, I. Goshev, J. Mihály, Effect of amine functionalization of spherical MCM-41 and SBA-15 on controlled drug release, J. Solid State Chem., 184 (2011) 1201–1207.
[39] Q. Qin, K. Liu, D. Fu, H. Gao, Effect of chlorine content of chlorophenols on their adsorption by mesoporous SBA-15, J. Environ. Sci., 24 (2012) 1411–1417.
[40] A. Deryło-Marczewska, M. Zienkiewicz-Strzałka, K. Skrzypczyńska, A. Świątkowski, K. Kuśmierek, Evaluation of the SBA-15 materials ability to accumulation of 4-chlorophenol on carbon paste electrode, Adsorption, 22 (2016) 801–812.
[41] M. Zienkiewicz-Strzałka, A. Deryło-Marczewska, R.B. Kozakevych, Silica nanocomposites based on silver nanoparticles-functionalization and pH effect, Appl. Nanosci., 8 (2018) 1649–1668.